water

MDPI

Article

Holocene Evolution of the Burano Paleo-Lagoon (Southern Tuscany, Italy)

Maurizio D'Orefice [1], Piero Bellotti [2], Adele Bertini [3], Gilberto Calderoni [4], Paolo Censi Neri [1], Letizia Di Bella [5,*], Domenico Fiorenza [1], Luca Maria Foresi [6,7], Markella Asimina Louvari [8], Letizia Rainone [3], Cécile Vittori [9], Jean-Philippe Goiran [10], Laurent Schmitt [9], Pierre Carbonel [10], Frank Preusser [11], Christine Oberlin [12], Francesca Sangiorgi [13] and Lina Davoli [5]

1 Italian Institute for Environmental Protection and Research, ISPRA, Department for the Geological Survey of Italy, 00144 Rome, Italy; maurizio.dorefice@isprambiente.it (M.D.); paolo.censineri@isprambiente.it (P.C.N.); domenico.fiorenza@isprambiente.it (D.F.)
2 AIGeo, Italian Association of Physical Geography and Geomorphology, c/o Department of Earth Sciences, Sapienza, University of Rome, 00185 Rome, Italy; piero.bellotti@gmail.com
3 Department of Earth Sciences, University of Florence, 50121 Florence, Italy; adele.bertini@unifi.it (A.B.); letizia.rainone@stud.unifi.it (L.R.)
4 Institute of Environmental Geology and Geoengineering, CNR, c/o Department of Earth Sciences, Sapienza, University of Rome, 00185 Rome, Italy; gilberto.calderoni@uniroma1.it
5 Department of Earth Sciences, Sapienza, University of Rome, 00185 Rome, Italy; lina.davoli@uniroma1.it
6 Department of Physical sciences, Earth and environment University of Siena, 53100 Siena, Italy; luca.foresi@unisi.it
7 Institute of Geosciences and Earth resources, CNR, c/o Research Area of Pisa, 1–56124 Pisa, Italy
8 Faculty of Geology and Geoenvironment Department of Historical Geology and Paleontology, National and Kapodistrian University of Athens, 15784 Athens, Greece; melinaluvari@geol.uoa.gr
9 Laboratoire Image Ville Environnement (LIVE), UMR 7362, University of Strasbourg, Faculté de Géographie et d'Aménagement, 67083 Strasbourg CEDEX, France; cecile.vittori@live-cnrs.unistra.fr (C.V.); laurent.schmitt@unistra.fr (L.S.)
10 Archéorient, UMR 5133 Maison de l'Orient et de la Méditerranée, Centre National de la Recherche Scientifique/Université of Lyon 2, 7 rue Raulin, 69007 Lyon, France; jean-philippe.goiran@mom.fr (J.-P.G.); carbonel@free.fr (P.C.)
11 Institute of Earth and Environmental Sciences, Albert-Ludwigs, University of Freiburg, 79104 Freiburg, Germany; frank.preusser@geologie.uni-freiburg.de
12 CNRS, French National Centre for Scientific Research, UMR 5138 ArAr, Lumière University Lyon 2, Claude Bernard University Lyon 1, 69622 Villeurbanne, France; christine.oberlin@univ-lyon1.fr
13 Department of Earth Sciences, Marine Palynology and Paleoceanography, Utrecht University, 3584 CB Utrecht, The Netherlands; F.Sangiorgi@uu.nl
* Correspondence: letizia.dibella@uniroma1.it

Received: 3 February 2020; Accepted: 26 March 2020; Published: 1 April 2020

Abstract: The study of Burano paleo-lagoon—Wetland of International Value, has allowed us to better define and extend the reconstruction of the Holocene paleoenvironmental evolution of the paleo-lagoons previously studied, located on the Tyrrhenian coast in central Italy. The investigated area is located in Southern Tuscany near the Burano Lake. The area was investigated by means of field surveys, historical maps, 16 coring, sedimentological, palynological and microfaunal analyses (foraminifera and ostracods), combined with robust geochronological control provided by 52 datings (^{14}C and OSL). The study allowed us to reconstruct the environmental and morphological evolution of the Burano paleo-lagoon during the last 8000 years and to hypothesize a Rise Sea Level (RSL) curve. In this context, 5 main evolutionary phases have been recognized. (1) before 7.5 ka BP in the southern-eastern part, an open lagoon developed; (2) ~6 ka BP a barrier-lagoon system develops throughout the entire area and the lagoon progressively changed from open to closed one; (3) ~5 ka

BP the width of the lagoon increases and a lacustrine facies appears along the entire axis of the coastal basin; (4) ~4 ka BP the lacustrine facies shows a discontinuous distribution respect to the previous phase; (5) during the last 4 ka the lacustrine facies disappear and the lagoon turns into a wetland area.

Keywords: Holocene; coastal lagoon; geochronology; sea level change; bio-indicators; Mediterranean Sea

1. Introduction

Although lagoons are environments that develop and become extinct in geologically short times, their sediments often constitute an important data archive relating to rapid events of considerable impact on the coastal area, which can also derive from variations on a global scale. The morphological and dynamic characteristics of the lagoons are extremely variable [1] according to the regional setting, tidal range and sediment availability. The development and evolution of the Holocene lagoons, mostly still active, were strongly influenced by the glacioeustatic sea level rise. During this period, in many cases the lagoons first developed within an incised valley [2] when the transgressive phase was still active. Later, they changed in shape, size and hydrodynamic characters when they reached almost sea level still stand [3–8]. Even shorter-term climatic variations [9] have often influenced the lagoon systems due to changes in coastal hydrodynamics and freshwater inflow [10,11].

The Tyrrhenian coast of the central Italian Peninsula (Figure 1), prone to a microtidal regime, is characterized by differently developed Holocene beach-dune systems bordering landward small-depressed areas. Until the nineteenth century, these areas were constituted of wetlands, lakes and lagoons. The land reclamations, between the end of the nineteenth to the first half of the twentieth century, transformed some coastal basins into cultivated or urbanized back dune plains. However, in some cases wide coastal lakes such as the ones located in the Southern and Northern Latium (M. Circeo promontory and Lido di Tarquinia respectively) have persisted until today. The Holocene history of some of these plains, that are locally close to river mouths (i.e., Tiber and Garigliano), has also been studied because of their geoarchaeological and historical importance [12–19]. The study of the Burano paleo-lagoon has allowed us to better define and extend the reconstruction of the Holocene paleoenvironmental evolution of the paleo-lagoons previously studied along the Latium coast from the Campania to the Tuscany regions. The study is very relevant because, unlike the extensive literature on meso and macrotidal estuarine systems, it highlights the Holocene evolution of a microtidal lagoon system. This system evolved into a tectonically stable area, not influenced by the proximity of important river mouths.

Similar studies were conducted in other areas of the Mediterranean Sea characterized by the presence of Holocene deltas and/or the ancient ports [20–29].

This paper focuses on the Burano paleo-lagoon that until 1830, extended for about 13 km along the Southern Tuscany coast between the Chiarone River mouth and the Ansedonia Promontory (Figure 1). It was possible to access and carry out the surveys only in part of the area where the portion of the paleo-lagoon stretching parallel to the coast for about 8 km, partly to the WNW and partly to ESE of the present-day Burano Lake. After the reclamation, the Burano Lake is what remains of the ancient lagoon. The lake, together with the neighbouring areas, is part of a Natural State Reserve. The area is also a Site of Community Importance (SCI IT51A0031), a Special Protection Zone (SPZ IT51A0033) and a Wetland of International Value (Ramsar Conventions on Wetlands). The purpose of the study is the Holocene reconstruction of the Burano paleo-lagoon evolution by means of facies analysis and stratigraphic relationships of the sedimentary bodies. The acquired data also allow us to hypothesize an RSL rise curve.

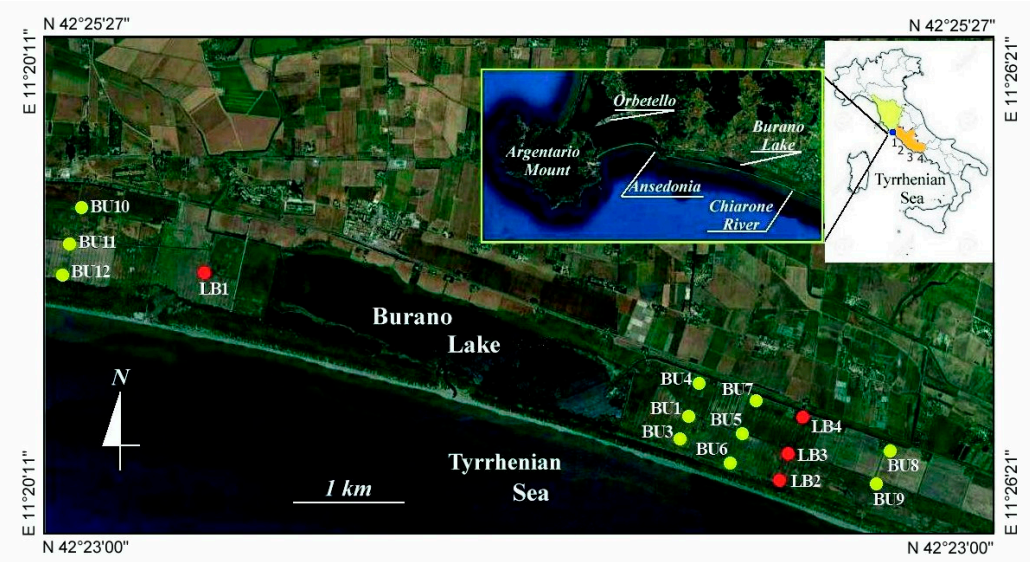

Figure 1. Location of the studied area. The position of the continuous (red dot) and percussion (yellow dot) drillings is indicated. The regions Tuscany (yellow) and Latium (orange) are indicated in the box at the top right. The numbers indicate the position of Lido di Tarquinia (1), Tiber river mouth (2), M. Circeo promontory (3) and Garigliano river mouth (4). From Google Earth image 2019. WGS84 Geographic Coordinate System refers to the vertices.

2. Regional Setting

From a geological point of view, the study area falls inside a narrow coastal belt, where Quaternary marine-coastal sediments outcrop, confined to the N and NW by hills made up of the pre-Quaternary substrate, which is progressively downthrown seaward by normal faults. The substrate is made up of lithotypes of the Tuscan metamorphic basement, on which intensely deformed Meso-Cenozoic sedimentary units tectonically overlap (Ligurian *l.s.* and the Falda Toscana Auct. units) [30,31]. Upper Miocene sediments follow upwards [30–32]; these sediments were deposited during the extensional phase related to the opening of the Tyrrhenian basin [33] and references therein Ref. [34]. The development of Pleistocene Vulsino volcanism, which is a few tens of kilometres from the study area, is linked to the same extensional phase [31].

3. Materials and Methods

In order to reconstruct the Holocene evolution of the Burano paleo-lagoon, at first a geomorphological analysis was carried out. Successively stratigraphical, sedimentological and geochronological analyses were conducted on sixteen cores drilled in the area (Figure 1). Moreover, palynological and microfaunal analyses were performed on selected cores in base of their chronology and sedimentary features.

3.1. Geomorphology

Historical maps relative to nineteenth century, bibliographic-cartographic literature, satellite images (Google Earth 2018) and aerial photos (1990) and field surveys (2016–2017) were utilized for the geomorphological analysis of the study area.

3.2. Lithology

Mechanical drillings and sampling—12 percussion and 4 mechanical rotary cores were carried out. The first ones (label BU1-12) were drilled by means of a coring system produced by AFgtc s.r.l. [35,36]. Both equipment and technique were suitable for the recovering of continuous cores, in which the sedimentary structures were preserved. The cores are 4–5 m long except for the core BU2,

which is only 0.80 m long. Its position coincides with BU3 and is not shown in Figure 1. The second ones (label LB1-4) were drilled by the Geoambiente soc. Coop. a.r.l. company, which performed archaeological cores for the Special authority for the archaeological heritage of Rome and several dozen geomorphological cores in the Tiber delta (ANR-POLTEVERE, ERC Portus-Limen). The mechanical drill-coring machine is equipped with a casing to prevent the hole from collapsing during the drilling operations. Sediment cores were retrieved and emptied without water by using a hydraulic extruder in order to avoid any kind of contamination and/or disturbance. This method provides continuous and deep core reaching depths between 6 and 15 m from the ground level. The lithology was described for all cores, considering a core stretching/shortening error, and sediment samples were collected for the sedimentological analyses. The samples were numbered indicating the depth in centimetres from the core top. SEM and diffractometric analyses were performed.

3.3. Geochronological Analysis

^{14}C dating was carried on 22 samples from cores BU1, 4, 5, 7, 10, 11, and 12. In LB cores, 25 AMS ^{14}C and 5 datings by Optically Stimulated Luminescence (OSL) were carried out.

In BU cores, dating was performed on plant remains ranging from herbs to variably altered woody debris, that had been previously decontaminated to remove carbonates, as well as acid- and alkali-soluble organics. The residues were then burned, and the resulting CO_2 was used for the synthesis of benzene, the means for the ^{14}C analysis using Liquid Scintillation Counting (LSC). The conventional ages, corrected for the C isotope fractionation to $\delta^{13}C = -25‰$ and calculated according to Stuiver & Polach [37], are reported in year BP (present time set at 1950). The conventional ages were calibrated according to Ref. [38]) and are given as calibrated years before the present (calibrated year BP). The uncertainties of both the conventional and calibrated ages are at the level of ± 1σ (i.e., 68% probability).

The radiocarbon datings relative to sediments in LB cores were mainly performed on *Posidonia* fibres, wood, plant remains and charcoal as well as occasionally on organic matter and shell. Charcoal and wood undergo an acid-base-acid pre-treatment (ABA). *Posidonia*, plant material and other organic matter are only treated with acid. Each acid or base wash is followed by several rinses with Merck Millipore MilliQ™ (Darmstadt, Germany) ultrapure deionized. After the final rinse, samples are dried prior the combustion. The standard pre-treatment method for shells involves surface cleaning by air abrasion with aluminium oxide powder to remove the outer surface and rinsing with ultrapure water. The sample is then dried. All glassware used is baked out at 500 °C prior to use for a minimum of 3 h to remove any organic contaminants. A few milligrams of the sample in solid form were placed in clean tin capsules and weighed. They were then combusted in an Thermo Finnigan Flash EA 1112 (San Jose, CA, United States) elemental NC analyser under a helium stream in the presence of copper oxide at 980 °C. The CO_2 produced in the combustion or by reacting in vacuo with phosphoric acid for the shell, was transferred to a glass ampoule, which was then sealed and sent to the Laboratory for Carbon 14 Measurement (LMC14) at Saclay (France). There, the CO_2 gas was reduced to solid graphite and measured by the Accelerator Mass Spectrometer or AMS (NEC tandem accelerator of 3MV), labelled "Artemis". The δ^{13} C values reflect the original isotopic composition in the sample only very roughly because the graphitisation process and the AMS spectrometer (unlike normal mass spectrometer) introduces significant isotopic fractionation.

Optical Stimulated Luminescence (OSL) dating of quartz extracts followed standard preparation techniques (chemical pretreatment, density separation, HF etching (cf. [39]). Measurements with the Single Aliquot Regenerative Dose (SAR) protocol [40] were done on a Freiberg Instruments Lexsyg Smart (Freiberg, Germany) device [41]. A preheat at 210 °C for 10 s was used and stimulation was for 50 s at 125 °C (detection at 380 nm). The distributions of the equivalent dose (D_e) expressed in grays (Gy), for most samples show a positive skewness, why the Minimum Age Model [42] was applied. For one sample (LB4), the D_e values spread from 50 Gy to more than 400 Gy without a distinct population and this sample is considered not datable. The concentration of dose-rate relevant elements was done by

high-resolution gamma spectrometry (cf. [43]). Ages were calculated using ADELE-v2017 software (add-ideas.de).

3.4. Sedimentological Analysis

A total of 37 clastic sediment samples were taken from BU cores and analysed, except of BU2 core due to its short length.

A basic sedimentological description was carried out on all the cores, highlighting the main sedimentary structures. Sieving was carried out for the coarser fraction (0.074 mm), while the finest one was determined using the densiometric technique. Samples were classified based on gravel-sand-silt-clay ratio according to the Folk classification scheme [44]. Moreover, 136 non-organic sediment samples were also taken from LB cores. For their analysis, about 30 g of dry bulk sediment were deflocculated in 2.5% sodium hexametaphosphate solution for 24 h before being wet sieved (2 mm and 63 μm). The dried coarse (>2 mm) and sandy (2 mm to 63 μm) fractions were weighted and the fine fraction (<63 μm) calculated to discriminate textural groups (according to gravel-sand-mud triangular diagrams described by Folk [44]).

3.5. Microfaunal Analysis

Foraminiferal analyses were performed on BU1, 3, 5 and 7 cores, while Ostracoda were studied on samples from all LB cores.

3.5.1. Foraminifera

For this purpose, 21 samples from BU1, 14 samples from BU3, 32 samples from the BU5 and 30 from the BU7 cores were collected, with different sampling resolution, giving special emphasis on the lithological changes. For each sample, 50–100 g of sediment was soaked, treated with hydrogen peroxide, washed over a 63 μm sieve and then oven-dried at 50 °C. Qualitative analyses was conducted on all samples while quantitative and statistical analysis was very difficult to carry out for the scarcity of the foraminiferal content and the holigothipic feature characterizing the samples. In particular, quantitative analysis was performed when the fauna was sufficiently present and split in aliquots containing at least 200–300 benthic specimens. Species diversity was quantified considering the number of taxa occurred in the samples (S) [45] and, where the count was possible, Shannon Weaver (H) and Fisher α-index were calculated using the PAST (PAlaeontological STatistics) version 1.38 data analysis package [46]. In each sample, between 3 and 38 taxa were identified, most of them displaying very low frequencies (1–4 individuals/sample). For generic attributions of benthic foraminifera see Ref. [47]. Taxonomic identifications at species-level were based on [48–50] and complied with the latest name list of the online database of the World Register of Marine Species [51]. The distinction of different benthic foraminiferal biofacies throughout the cores relies chiefly on the ecological preferences of the most abundant species and microfaunal diversity.

3.5.2. Ostracoda

One hundred and thirty-six sediment samples from LB cores were analysed for ostracods (LB1:65, LB2:36, LB3:41 and LB4:21). Ostracods were recovered from 98 samples (LB1:45, LB2:10, LB3:36 and LB4:11) and 50 species were identified. The sandy fraction of the texture samples was dry sieved and the ostracods were extracted from fine to medium sand-sized sediment residues (500 to 125 μm). Up to 100 ostracods were picked using a stereomicroscope (Diaspore model from Nachet). The best-preserved ostracod shells were identified using Environmental Scanning Electron Microscopy (ESEM) images [52] with reference to [53–59] and the taxonomic attribution follows [51]. The ostracod density was expressed as the number of valves/g and the species richness (diversity) as the number of species in each sample. The ostracod taxa were divided in 5 ecological groups according to their salinity tolerance and their habitat: freshwater to low brackish, brackish, lagoonal coastal, phytal coastal and marine (Table 1).

Table 1. Ecological groups with the related taxa (in bold the common taxa > 5 valves).

Ecological Groups	Taxa (Binomial Nomenclature)
Freshwater to low brackish	*Candona* sp. ***Candona angulatata*** ***Darwinula stevensoni*** *Herpetocypris* sp. *Heterocypris salina* *Ilyocypris* sp. *Limnocythere inopinata* *Paralimnocythere* sp. *Pseudocandona* sp.
Brackish	***Cyprideis torosa*** ***Loxoconcha elliptica***
Lagoon/coastal	***Loxoconcha* sp.** ***Xestoleberis communis*** ***Xestoleberis dispar***
Phytal coastal	***Aurila* sp.** ***Aurila woodwardii*** ***Bairdia mediterranea*** *Callistocythere pallida* ***Cushmanidea turbida*** ***Cytheretta* sp.** *Cytheridea neapolitana* ***Hiltermannicythere rubra*** *Leptocythere* sp. ***Leptocythere bacescoi*** *Leptocythere* cf. *ramosa* ***Leptocythere fabaeformis*** *Microcytherura angulosa* *Microcytherura fulva* ***Neocytherideis fasciata*** *Neocytherideis (Sahnia) subulata* *Paracytheridea depressa* *Procytherideis* (*Neocytherideis) subspiralis* *Sagmatocythere littoralis* *Semicytherura* sp. *Semicytherura* aff. *rara* *Semicytherura amorpha* *Semicytherura incongruens* *Semicytherura sulcata* *Urocythereis favosa*
Marine	*Carinocythereis whitei Costa punctatissima* *Cytheropteron latum Eucythere curta* *Eucytherura angulata* *Jugosocythereis* sp. ***Paracytherois mediterranea*** *Paradoxostoma bradyi*

3.6. Palynological Analysis

Forty-eight samples were taken between 0 and 430 cm from the BU1 core. Twenty-four samples were processed at the Palynological Laboratory of the University of Florence. An additional 24 samples were processed at laboratory of University of Utrecht as part of an Erasmus plus traineeship. Both laboratories used the exact same standard procedure for palynological processing. One *Lycopodium clavatum* tablet containing a known amount of spores was added to each exactly weighted dried sample to determine palynomorph concentrations. The samples, ~1.00 to 3.3 g in weight, were treated

with 30% HCl, cold 38% HF, and briefly with KOH. Residues were then sieved in an ultrasonic bath using a 10 µm polymer mesh. Thirty-eight mobile slides were mounted using glycerol and analysed using optical microscopes. Slides are very rich in both pollen and Non-Pollen Palynomorphs (NPPs). In particular, land-derived palynomorphs include pollen, fungal remains (e.g., spores, hyphae, and fruiting bodies) and embryophyte spores. Freshwater palynomorphs include algal zygospores, especially Desmidiaceae (e.g., *Cosmarium*) and Zygnemataceae (e.g., *Mougeotia*), invertebrate mandibles, aquatic fungi, *Pediastrum* and *Botryococcus* algae. Marine palynomorphs include cyst of dinoflagellates, and foraminifer linings. The preservation of both pollen grains and NPPs is generally good; in fact, degraded, corroded or broken remains are very rare; moreover, there is no evidence for reworking of palynomorphs.

The results of the pollen analysis are summarized in a pollen percentage diagram including two main groups, i.e., Arboreal (AP) and Non Arboreal (NAP) taxa; here the main percentage sum is based on terrestrial pollen excluding NPPs. Moreover, on the right of the summary pollen diagram, the occurrence of selected NPPs is marked.

4. Results

4.1. Geomorphology

A depression parallel to the coast with WNW-ESE trend, limited landward by Pleistocene sandstone deposits and seaward by a coastal dune system, characterizes the studied area. Near the depression, the sandstone deposits rise to about 20 m a.s.l. Two ridges distant from each other, about 100 m and both approximately 70–80 m wide, constitute the dune system (primary and secondary dune). This system is confined between depression containing the paleo-lagoon and the present backshore. The maximum altitude of the outer dune system is close to 8 m a.s.l. and a dense shrub vegetation of Mediterranean maquis covers the secondary dune. The back-barrier is about 1 km wide. Before the nineteenth-century reclamation, the depression was a wetland periodically submerged; the Fosso Melone and the Fosso del Chiarone rivers flowed into the depression, in the central and eastern part, respectively (Figure 2). Currently, the depression is almost flat and at some decimeters below sea level. The depression is crossed by several reclamation canals and includes the Burano Lake, the only submerged area after the old lagoon reclamation. The lake is about 3.5 km long, 0.5 km wide and covers an area of about 1.5 km^2, with a maximum depth of about 1 meter. An inlet, located at the centre of the outer side, connects the lake to the sea. Washover fans are particularly evident in the north-western area of the lake.

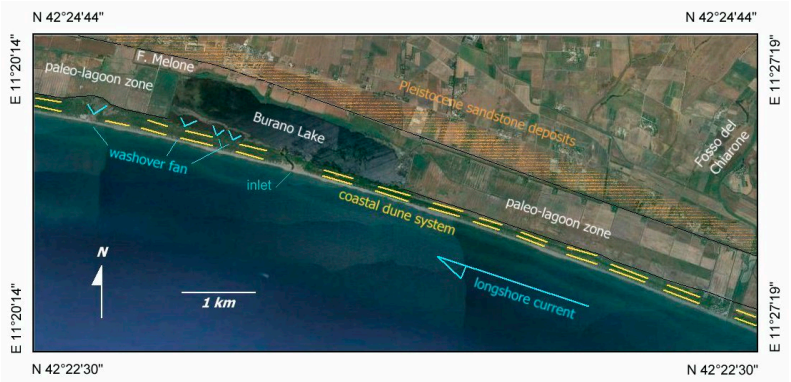

Figure 2. Geomorphological sketch map. The Fosso del Chiarone (river), which today flows into the sea, flowed into Lake Burano before the reclamation works. The washover fans indicate in the sketch are inactive today. From Google Earth image 2019. WGS84 Geographic Coordinate System are referred to the vertices.

4.2. Lithological Units

Five lithological units (Figure 3a,b) were recognized based on the cores.

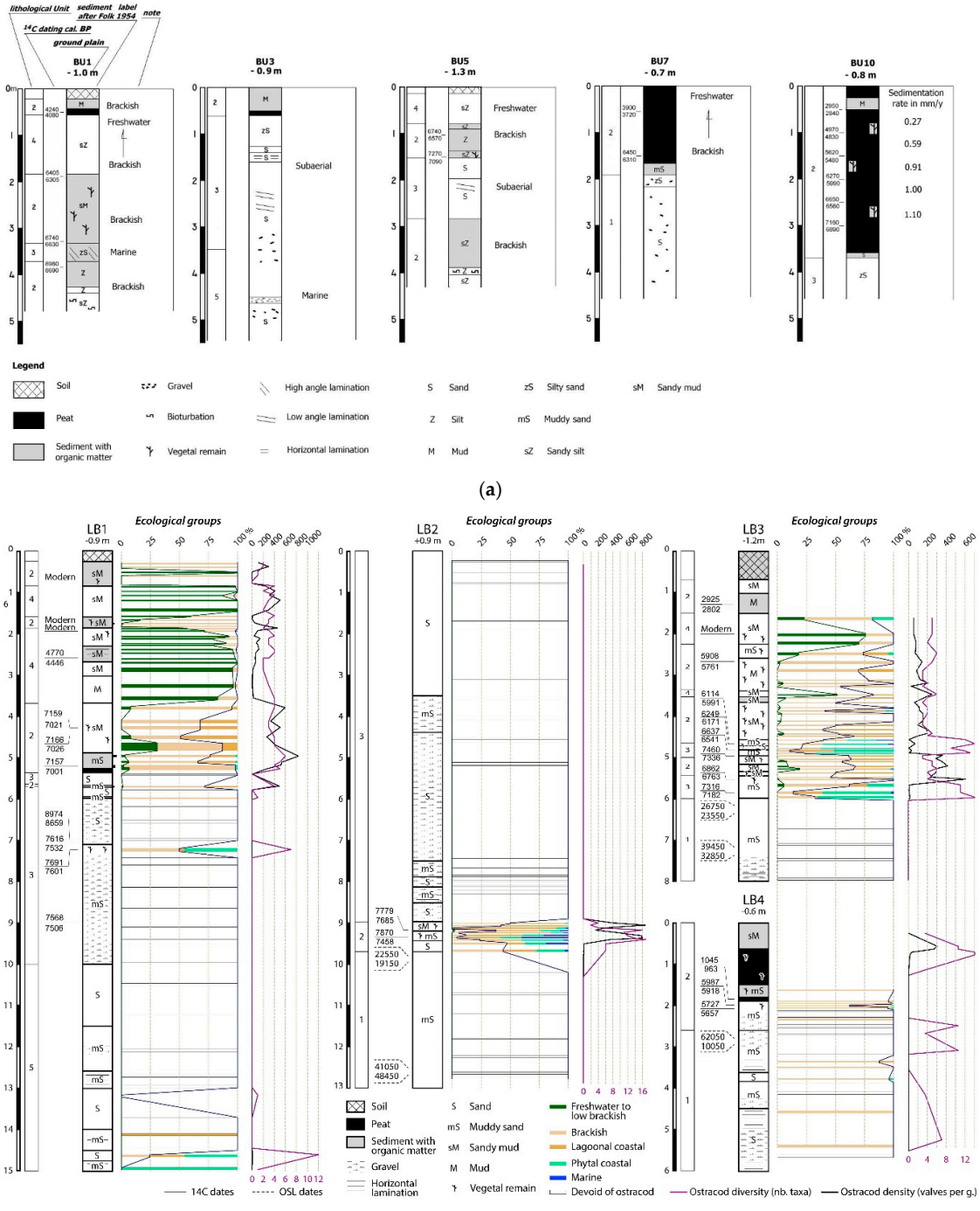

Figure 3. (**a**) Litho-stratigraphy and environmental evolution along BU1, 3, 5, 7, 10 percussion drillings. In BU10 core, the sedimentation rates in the peats are reported. (**b**) Litho-stratigraphy and ostracod ecological groups distribution along LB1, 2, 3, 4 continuous drillings. Age cal BP.

- Unit 1—Ocher and locally cemented quartz silty sands (zS) constitute this unit. Rare fine gravel with occasional centimetric pebbles and local plane-parallel lamination are present. The medium-sorted sediment shows uni or bimodal grain-size distribution. This unit outcrops along the inner edge of the depression and it was intercepted at the base of the BU4, 7 and 8, LB 2, 3 and 4 cores. The unit was crossed for about 3 m without ever reaching the bottom.
- Unit 2—It is a complex lithology unit mainly consisting of: soft peats, sandy mud (sM), mud (M), silt (Z) and muddy sand (mS) with abundant organic matter. Some thin levels with shell debris; are present more frequently in the lower part of the unit. They show a high silt content and are locally bioturbated. There are remains of *Posidonia* and undecomposed vegetal matter, occasional bivalve fragments and thin-shell gastropods. In the upper part, the unit is characterized by black-brown decametric thick soil outcropping into the depression. The unit was intercepted in the central and upper part of almost cores with a thickness ranging from 0.50 to over 3.0 m.
- Unit 3—It is made up of fine to medium-coarse greyish, more rarely yellowish, no diagenized feldspathic quartz sands (S). Sands are well sorted with a unimodal grain size distribution curve. Muddy sand (mS) and silty sand (zS) are more rarely present. Horizontal and medium-low angle plane-parallel laminations are present and centimetric to decimetric dark levels with femic minerals (in particular augite) were observed too. SEM and diffractometric analyses showed rare garnets, amphibole, pyrite, ilmenite, titanite and magnetite. There are locally present oblate or flattened pebbles, rare fine gravel levels and bivalves with complete shell or more frequently fragmented. This unit was intercepted mainly in the drills closest to the sea (where sometimes it represents the only body intercepted) with maximum thicknesses of about 7 m (LB2) and with more reduced thicknesses in the central ones; it is not present in the inner cores except BU10. Locally, this unit is interbedded to Unit 2 where it sometimes shows a high angle lamination.
- Unit 4—Whitish $CaCO_3$ enriched silt (Z), scarce fine sand (S) and a bioclastic fraction characterize this unit. SEM and diffractometric analyses showed a composition constituted mainly of euhedral calcite crystals and subordinately secondary of gypsum. Downwards rare dark horizontal laminations were observed. This unit was intercepted in the upper part of the cores drilled in the central sector of the depression. The thickness is greater northward where it reaches about 2 m (LB1). In most parts of the cores, the whitish silt is interbedded with thin blackish peaty levels and in any case is always embedded in the Unit 2.
- Unit 5—This unit consists of medium to fine incoherent silty sand (zS) and muddy sand (mS). Moreover, there are horizontal plane-parallel laminations, rare gravel constituted of flat grains rare oxidized foraminifera and shell debris. This unit was intercepted, below Unit 3, in LB1 core for a thickness of about 7 m without ever reaching the bottom, and in BU3 core.

For the geochronological data, see Tables 2 and 3.

Table 2. Radiocarbon datings (LB samples [52]).

Sample Identifier	Core # (Depth in Core, m)	Material	Conventional ^{14}C Age (Year BP)	Calibrated Age (Calibrated Year BP)	$\delta\,^{13}C^{(2)}$ (‰, *vs.* SMOW (Standard Mean Ocean Water))
Rome-2334	BU-1 (0.45–056)	sandy peat	3775 ± 40	4200–4080	−21.7
Rome-2335	BU-1 (1.82–1.89)	clay peat	5770 ± 40	6405–6305	−26.0
Rome-2336	BU-1 (3.10–3.19)	silt peat	5860 ± 40	6740–6630	−24.8
Rome-2337	BU-1 (3.59–3.64)	clay peat	7940 ± 50	8980–8690	−23.1
Rome-2338	BU-4 (0.50–0.60)	peat debris	1010 ± 40	960–850	−23.7
Rome-2339	BU-4 (1.0–1.1)	peat level	3570 ± 40	4090–3920	−25.0
Rome-2340	BU-4 (1.75–1.85)	clay peat	5940 ± 50	6860–6670	−25.8
Rome-2341	BU-5 (0.98–1.08)	peat debris	5860 ± 45	6740–6570	−23.4
Rome-2342	BU-5 (1.44–1.54)	silt clay	6280 ± 50	7270–7090	−24.9
Rome-2342•	BU-7 (0.50–0.60)	peat level	3550 ± 40	3900–3720	−22.5

Table 2. *Cont.*

Sample Identifier	Core # (Depth in Core, m)	Material	Conventional ^{14}C Age (Year BP)	Calibrated Age (Calibrated Year BP)	$\delta\ ^{13}C^{(2)}$ (‰, *vs.* SMOW (Standard Mean Ocean Water))
Rome-2343	BU-7 (1.44–1.57)	clay peat	5620 ± 45	6450–6310	−23.2
Rome-2349	BU-10 (0.50)	peat level	2790 ± 40	2950–2840	−22.9
Rome-2360	BU-10 (1.00)	peat level	4320 ± 40	4970–4830	−24.1
Rome-2364	BU-10 (1.50)	peat level	4840 ± 40	5620–5480	−22.5
Rome-2361	BU-10 (2.00)	peat level	5310 ± 40	6270–5990	−24.1
Rome-2365	BU-10 (2.50)	peat level	5840 ± 40	6650–6560	−22.6
Rome-2350	BU-10 (3.00)	peat level	6115 ± 40	7160–6890	−25.0
Rome-2348	BU-11 (1.31–1.46)	clay peat	3830 ± 35	4290–4150	−23.4
Rome-2347	BU-11 (2.83–2.97)	silty peat	5270 ± 40	6170–5940	−24.3
Rome-2346	BU-11 (3.53–3.67)	clay peat	6445 ± 45	7430–7320	−25.1
Rome-2344	BU-12 (0.50)	peat level	3700 ± 40	4090–3930	−23.5
Rome-2345	BU-12 (1.00)	peat level	4560 ± 45	5320–5050	−24.2
Lyon-14228(sacA-49736)	LB1 (0.70)	Wood	Modern	Modern	Unavailable
Lyon-14223(sacA-49731)	LB1 (1.75–1.78)	Plant material	Modern	Modern	Unavailable
Lyon-15107(sacA-53026)	LB1 (1.93–1.96)	Plant material	Modern	Modern	Unavailable
Lyon-14224(sacA-49732)	LB1 (2.57)	Charcoal	4060 ± 30	4779–4446	Unavailable
Lyon-15109(sacA-53028)	LB1 (3.64–3.71)	Wood	6180 ± 30	7159–7021	Unavailable
Lyon-15110(SacA-53029)	LB1 (3.93–3.96)	Wood	6200 ± 30	7166–7026	Unavailable
Lyon-14226(sacA-49734)	LB1 (4.25–4.28)	Wood	6155 ± 35	7157–7001	Unavailable
Lyon-15117(SacA-53036)	LB1 (5.35–5.40)	Wood	7945 ± 35	8974–8659	Unavailable
Lyon-15108(sacA-53027)	LB1 (5.47)	*Posidonia*	7095 ± 40	7616–7532	Unavailable
Lyon-14227(sacA-49735)	LB1 (5.56–5.62)	*Posidonia*	7190 ± 40	7691–7601	−14.66
Lyon-15111(sacA-53030)	LB1 (7.13)	Wood	6640 ± 30	7568–7506	Unavailable
Lyon-15112(SacA-53031)	LB2 (7.67–7.70)	*Posidonia*	7275 ± 35	7779–7685	Unavailable
Lyon-14229(sacA-49737)	LB2 (7.78–7.81)	*Posidonia*	7350 ± 40	7670–7458	−14.51
Lyon-14231(sacA-49739)	LB3 (0.40-0.43)	Organic matter	2775 ± 30	2925–2802	−26.14
Lyon-14230(sacA-49738)	LB3 (0.72–0.75)	Plant material	Modern	Modern	Unavailable
Lyon-15113(SacA-53032)	LB3 (1.03–1.06)	Shell	5095 ± 30	5908-5761	Unavailable
Lyon-14232(sacA-49740)	LB3 (3.06–3.09)	*Posidonia*	5655 ± 35	6114–5991	−14.13
Lyon-15118(SacA-53037)	LB3 (3.12)	*Posidonia*	5770 ± 30	6249–6171	Unavailable
Lyon-15119(SacA-53038)	LB3 (3.30–3.34)	Wood	5775 ± 30	6637–6541	Unavailable
Lyon-15114(SacA-53033)	LB3 (3.44–3.48)	Charcoal	6500 ± 30	7460–7336	Unavailable
Lyon-15115(SacA-53034)	LB3 (3.86–3.89)	Shell	6345 ± 30	6862–6763	Unavailable
Lyon-14233(sacA-49741)	LB3 (4.33–4.39)	Charcoal	6335 ± 35	7316–7182	Unavailable
Lyon-14234(sacA-49742)	LB4 (1.00–1.03)	Plant material	1085 ± 35	1045–963	Unavailable
Lyon-15116(SacA-53035)	LB4 (1.12–1.15)	Plant material	5190 ± 30	5987–5918	Unavailable
Lyon-14235(sacA-49743)	LB4 (1.18–1.21)	Wood	4970 ± 30	5727–5657	Unavailable

Table 3. OSL (Optically stimulated Luminescence) datings [52].

Sample	Depth (cm)	K (Bq/kg)	Th (Bq/kg)	U (Bq/kg)	W_{meas} (%)	W_{eff} (%)	D-Q (Gy ka^{-1})	Grain size (μm)	N	Od	D_e OSL (Gy)	Age OSL (ka)
LB2-1	840	1320 ± 80	75.0 ± 4.9	46.4 ± 2.8	15.4	20 ± 5	5.22 ± 0.40	150–200	24	0.28	118.86 ± 7.52	22.8 ± 1.7
LB2-2	1115	1580 ± 160	69.9 ± 3.9	55.0 ± 3.0	13.0	20 ± 5	5.92 ± 0.47	150–200	25	0.22	276.15 ± 14.01	46.7 ± 3.7
LB3-1	478	1400 ± 80	68.3 ± 3.8	47.1 ± 2.9	12.5	20 ± 5	5.28 ± 0.31	200–250	27	0.17	142.98 ± 5.89	27.1 ± 1.6
LB3-2	585	1340 ± 130	67.2 ± 3.9	46.1 ± 2.7	13.7	20 ± 5	5.09 ± 0.44	200–250	21	0.25	193.97 ± 12.42	38.1 ± 3.3
LB4	210	1470 ± 120	96.1 ± 5.8	64.1 ± 4.0	11.6	20 ± 5	6.26 ± 0.33	150–200	24	0.60	70–400	12–64

4.3. Paleovegetational Context

Pollen data from BU1 core provide the floristic and vegetation history of Burano Lake during the last 8000 years (Figure 4). Thermophilous deciduous forest composed especially of *Quercus cerris* and *Q. pubescens* followed by other sub-Mediterranean taxa such as *Carpinus orientalis/Ostrya*, *Corylus*, *Quercus suber,* dominate the landscape in the lowlands and hilly areas. Here, Mediterranean vegetation shows less extension than the sub-Mediterranean one; its main taxon is *Quercus ilex,* followed by Ericaceae, *Olea*, *Phillyrea*, *Pistacia*, etc. Pollen data indicate the presence although with low percentages of *Abies*, *Betula* and *Fagus,* typical taxa of high altitude; among them, *Fagus* shows the more continuous record. Plants growing under greater control of local edaphic conditions include prevalently herbaceous taxa such as Amaranthaceae and Cyperaceae which possibly expanded especially on the lake shoreline.

Mediterranean taxa show some phases of increase, the most evident of them occurred between 8000 and 5860 BP. However, over the previous fluctuations, no dramatic vegetational changes were

pointed out throughout the pollen record also before 3775 BP, when a strong increase in herbaceous taxa occurred. In this context, Amaranthaceae exhibited at least two main phases of increase which possibly correspond to a decrease of the extension of the Burano paleo-lagoon.

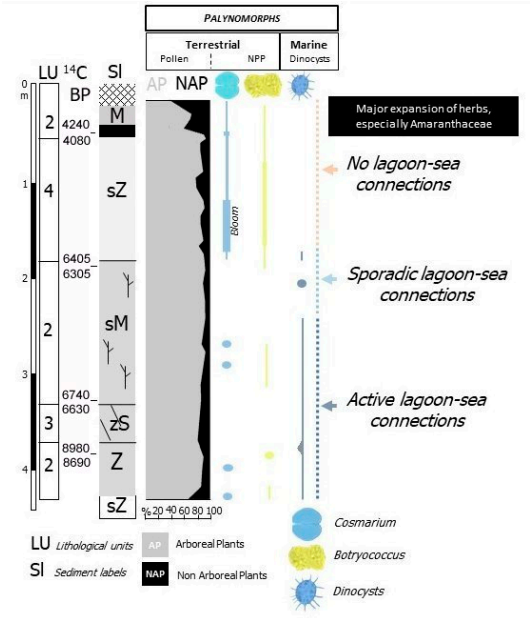

Figure 4. Summary of the palynological evidence from BU1 core. For the legend of sediment labels see Figure 3a. Age calibrated year BP.

4.4. Bio-Indicators of the Aquatic Paleoenvironmental Conditions in Each Units

Unit 1—*Ostracoda*: samples from LB cores are generally devoid of ostracods except for a few LB4 samples showing low ostracod density. The assemblages are highly dominated by the euryhaline taxon *Cyprideis torosa* monospecific or associated with scarce valves of brackish (*Loxoconcha elliptica*) or lagoon/coastal (*Xestoleberis dispar*) species. These assemblages, dominated by *C. torosa*, have low densities in semi-permanent waters of lagoon marginal areas [60,61].

Foraminifera: only oxidized shallow water foraminifera and rare molluscs fragments characterize this unit.

Unit 2—*Ostracoda*: in the LB cores, the samples are mainly characterized by a high ostracod density and a relatively low diversity (2 to 6 taxa). Ostracods are mainly composed of both brackish (*C. torosa* and *L. elliptica*) and lagoon/coastal (*X. dispar*) taxa with variable proportions, all three of which can be dominant or co-dominant. They are occasionally associated with a few phytal coastal (*Aurila* spp. and *Leptocythere* spp.) and/or freshwater to low brackish specimens (*Candona angulata* and *Darwinula stevensoni*); this assemblage is characteristic of an open lagoon environment. The abundance of *X. dispar* indicates polyhaline conditions with substantial seawater inputs [53,62]. In the LB2 core, between 915 and 970 cm, the samples have a low ostracod density and a high diversity (7 to 17 taxa). These assemblages are dominated by *C. torosa*, *X. dispar* or the marine species *Paracytherois mediterranea*, mainly associated with *L. elliptica*, lagoon/coastal (*Loxoconcha* sp. and *Xestoleberis communis*) and phytal coastal taxa (main species are *Cushmanidea turbida* and *Urocythereis favosa*). Sporadic specimens (1 to 3 valves) of about 20 other coastal and marine taxa are reported. The abundance and diversity of marine and coastal taxa is common in euhaline to polyhaline lagoon environment with a strong seawater influence typical of sandy bar inlets surroundings [61,63]. In core LB1, between 20–40 cm, 160–190 cm and 520–530 cm occurs a bispecific assemblage dominated by *C. torosa* associated with *L. elliptica* characteristic of confined lagoons [61,63–66]. The association of these two euryhaline species suggests intra- and inter-annual variations in salinity. In the LB4, two samples (165–168 cm and

233–238 cm) are monospecific with scarce valves of *C. torosa*, which could indicate semi-permanent waters [60,61]. In core LB1, between 40 and 60 cm each sample contains only one reworked valve.

Foraminifera: they are mainly represented by brackish lagoonal assemblage containing an oligospecific fauna characterized by the high dominance of *Ammonia tepida* (75–91%) accompanied by few species (mainly *Haynesina germanica* 4–8% and *Porosononion granosum* 1–19%). The low diversity (S: 3 to 7 taxa, Fisher α-index: 0.4 to 5, H: 0.3 to 1.7) and the high dominance of *A. tepida*, a euryhaline species, are indicative of an enclosed brackish lagoon [67–71]. This assemblage is recorded in BU5 core, from 330 to 300 cm and from 122 to 81 cm, and in BU7 core, from 216 to the top. Towards the top of the unit (BU7: from 166 cm to the top) it is characterized by a clear transition towards freshwater conditions highlighted by a decrease of foraminiferal content. Similar environmental condition is recognized also in the upper part of the BU1 core (from 61 to 30 cm) where the assemblage is similar to that written above for the upper part and it is associated with abundant gastropods like *Hydrobia* spp. and *Planorbis* spp.; while at the lower part (bottom to 386 cm), more marine taxa (*Nonion* spp., *Triloculina* spp. and *Quinqueloculina* spp.) indicate a significant sea influence. This unit in BU1 core is also characterized by the presence of Characeae oogones and monassone spicules of porifers. In BU3 core, this unit is barren.

Palynology (NPPs): palynology was studied in core BU1. Between 426 and 371 cm depth, marine dinocysts are usually present although in low abundance compared to the terrestrial palynomorphs. In particular, at 387 cm dinocysts increase and are well represented by *Spiniferites mirabilis,* an indicator of warm-temperate conditions and *Lingulodinium machaerophorum,* often found in estuarine, coastal/neritic environments in modern sediments. *L. machaerophorum* thrives in nutrient-rich conditions and can reach high abundances in river-dominated marine areas [72]. Blooms of its motile form can cause toxic red tides. The other species found are typical of neritic to coastal warm-temperate environments, such as *Operculodinium centrocarpum*, *Operculodinium israelianum, Selenopemphix quanta, Spiniferites belerius, Spiniferites bulloides, Spiniferites membranaceous, Spiniferites ramosus*. Notably, typical oceanic taxa such as *Impagidinium* spp. are absent. Some foraminifer linings are also present; such organic test linings probably belong to calcareous benthic foraminifers, the occurrence of which indicates a shallow depositional environment, nutrient-rich waters and relatively more fully marine salinities. *Botryococcus* (Chlorophyceae, Chlorococcales/Tetrasporales), a fresh–brackish water colonial green algae is quite abundant. Throughout this interval, *Pseudoschizaea* (Incertae sedis) and some hemi-cells of the prevalent freshwater Desmidiaceae *Cosmarium* have also scattered occurrences. Terrestrial Fungi are always abundant. Between 332 and 188 cm, Fungi spores, *Pseudoschizaea, Botryococcus* and especially *Cosmarium* decrease markedly. Dinocysts also decrease toward the top of the interval. Some foraminifer linings are present. From 56 to 42 cm, marine dinocysts are absent whereas *Cosmarium*, *Botryococcus* and fungal spores are present.

Unit 3—*Ostracoda*: samples from LB2 core are devoid of ostracod fauna. Samples from LB3 core have a high ostracod density and a low specific diversity (9 to 14 taxa). The assemblages are slightly dominated by the euryhaline species *C. torosa* or the phytal coastal species *C. turbida* associated with brackish (*L. elliptica*), lagoon/coastal (*Loxoconcha* sp. and *Xestoleberis* spp.) and phytal coastal taxa (mainly *Aurila* spp., *Bairdia mediterranea, Cytheretta* spp., *Hiltermannicythere rubra*, *Leptocythere* spp., *Neocytherideis* spp., *Semicytherura* spp. and *U. favosa*). It can be associated with an open lagoon environment strongly influenced by seawater and the closeness of a sandy bar inlets. In the LB1 core, the samples are devoid of ostracods or contain one or two reworked valves except for one sample (720–730 cm) which has similar characteristics to the LB3 samples.

Foraminifera: in this unit the foraminiferal assemblage shows, in respect to the Unit 2, a clear decrease of lagoonal taxa (e.g., *Ammonia tepida* displays a decreasing trend from BU5-285 to BU5-283) and an increase of typical shallow marine species like miliolids (>22% *Quinqueloculina* spp. and *Triloculina* spp.), *Elphidium* spp. (4–8%) and *Rosalina* spp. (7–40%) [49,58,73]. This assemblage presents very few specimens but high diversity (S: 18 to 38 taxa, Fisher α-index: 6.0 to 20.4, H: 1.8 to 3.1). The environment related to Unit 3 can be associated with a lagoon affected by occasional marine

connection. This assemblage is recorded in BU5 core (from 300 to 132 cm) and in BU1 (from 370 to 320 cm) and BU3 (from 405 to 369 cm) cores where siliceous spicules of poriferas were found too. Moreover, it is characterized by abundant remains of molluscs (*Cardium* spp., *Glycimeris* spp., *Venus* spp. and tellinids) vermetids, bryozoans, coral algae and remains of echinoids. In BU3 core, the upper part of the unit, contains only reworked molluscs.

Palynology (NPPs): data have been collected from the BU1 core between 371 and 332 cm. Samples are mostly barren in NPP but also pollen probably due to the unfavourable lithology marked by a high content in sand. Marine dinocysts such as *S. belerius*, *S. membranaceous*, *S. ramosus* are present along foraminifera linings and *Pseudoschizaea*.

Unit 4—*Ostracoda*: samples from LB cores have a low ostracod density. In the LB1 samples, ostracods are low diversified (2 to 4 taxa) and highly dominated by the freshwater to low brackish species *C. angulata* mainly associated with a freshwater to low brackish (*D. stevensoni*) and/or a euryhaline species (*C. torosa*). *C. angulata* tolerate limnetic to mesohaline waters but clearly prefers slightly salty waters and are common in slightly brackish coastal ponds [70]. In the LB3 samples, ostracods are moderately diversified (5 to 6 taxa) and dominated by *C. torosa* mainly associated with freshwater to low brackish (*C. angulata*, *D. stevensoni* and *Limnocythere inopinata*) and brackish taxa (*L. elliptica*). These two assemblages are common in low brackish lagoon environment. In the LB3 core, *L. elliptica* which tolerates oligohaline to polyhaline waters and the dominance of *C. torosa* for which maximum productivity occurs at salinities between 2 and 16.5‰ [70] indicates slightly higher salinities than in the LB1 core.

Foraminifera: unlike ostracods, in this unit benthic foraminifera are rare or absent with a very low diversity (S: 3 to 4 taxa, Fisher α-index: <1, H: 0.3 to 0.7), advocating freshwater or low brackish conditions. It is recorded in BU1 core from 164 to 72 cm and in BU5 core from 91 cm to the top. Where it is associated with abundant gastropods (*Hydrobia* spp. and *Planorbis* spp.) and frequent oogones.

Palynology (NPPs): the interval between 188 and 56 cm of core BU1 shows some sporadic/rare presence of dinocysts (*Spiniferites* spp.) along with few hemi-cells of the freshwater *Cosmarium* and fresh–brackish water *Botryococcus* at the base. However, in the interval from 170 to 64 cm, a sudden change in the NPP assemblages occurs, marked by the increase of *Cosmarium* and *Botryococcus* as well as by the disappearance of dinocysts. In more detail, *Cosmarium*, shows an acme phase between 170 and 123 cm and *Botryococcus* is also well represented although in lower occurrence.

Unit 5—The samples include scarce reworked valves of coastal or lagoon ostracods. Only one sample, at bottom of LB1 core, present a low ostracod density with a high diversity (12 taxa). This assemblage is slightly dominated by the phytal coastal species *C. turbida* associated with lagoon/coastal (*Loxoconcha* sp. and *Xestoleberis* spp.), brackish (*C. torosa* and *L. elliptica*) and phytal coastal taxa (*B. mediterranea*, *Cytheretta* sp., *H. rubra*, *Semicytherura sulcata* and *U. favosa*). Rare tellinids and oxidized foraminifera are also present.

5. Discussion

5.1. Facies and Reciprocal Stratigraphic Relationships (Figure 5):

- Coastal Pleistocene facies (CP)—It is characterized by the lithological Unit 1 in which rare fragments of bivalves, oxidized shallow waters foraminifera and rare brackish and euryhaline ostracods have been found. The measured age varies between about 45 to about 20 ka BP. The lithology, the faunal content and datings, identify a generic coastal plain developed during the Upper Pleistocene.
- Lagoon Holocene facies (LgH)—It includes sediments that refer prevalently to the Unit 2 in which the faunal content consists of predominant brackish and lagoonal/coastal taxa. Sometimes these taxa are accompanied by species more suitable for freshwater environment. It is confirmed by the absence of foraminiferal assemblages in the upper part of the unit. The decrease of marine dinocysts confirm a minor lagoon-sea connection in the time. According to the composition and stratigraphical distribution of dinocysts a main seawater input is documented close to about 8 ka

BP (BU1 426 to 371 cm) whereas the marine influence progressively decreases until it disappears towards the more recent times. This facies develops mostly until 3.5 ka BP, even if locally, it is also present in more recent times (2.8–1.0 ka BP, Table 1). LgH facies is attributable to a coastal Holocene lagoon significantly influenced by the sea in the period before 6 ka BP even if phases of greater or less marine connection alternate over time. Using the calibrated ages in the BU10 core, where the organic sediments of this facies are more continuous and lacking clastic intercalations, the peat sedimentation rates were estimated (Figure 3a). These progressively decrease from 1.1 to 0.27 mm/year.

- Beach-dune Holocene facies (BdH)—It includes Unit 3 deposits characterized by the occurrence of prevalent marine bio-indicators; all previous evidences support the development of foreshore/dune, sand barrier environment and subordinately washover fans.
- Lacustrine Holocene facies (LH)—It corresponds to the whitish $CaCO_3$ enriched Unit 4. The faunal component is essentially made up of freshwater gastropods and freshwater/low brackish ostracods. NPPs as a whole, confirm a prevalent freshwater environment; indeed, the main components of the NPPs assemblages are *Cosmarium*, indicative of prevalent freshwater conditions and *Botryoccoccus*, which thrives in fresh–brackish waters. Notably, their abundances (especially that of *Cosmarium*) indicates a bloom around 5770 year BP (in BU1). Such bloom may indicate a sudden change in one or more environmental parameters such as nutrients (e.g., phosphorus and nitrogen), temperature or pH. It is also necessary to understand if the phenomenon was natural or anthropic-induced. *Cosmarium* and *Botryococcus* proliferate in oligo-to mesotrophic conditions, and therefore a sudden eutrophication episode can be excluded. The absence of other taxa such as *Pediastrum*, aquatic algae commonly present in freshwater habitats rich in mineral and organic nutrients confirms the oligotrophic conditions. Desmids are sensitive organisms and act as an indicator of water quality, concentration of chemical oxygen demand, nitrate and turbidity; *Botryococcus* can dominates (or be present) in relatively extreme environments which prevents for example the occurrence of *Pediastrum*; it is often present when water is clear, oligotrophic, eventually dystrophic [74–76]. All this evidence permits to define a freshwater depositional basin with clear and oligotrophic waters. Moreover, the abundance of calcite suggests medium-high pH waters and probably microbially induced calcium carbonate precipitation a phenomenon also associated with the so-called "Whitings" (e.g., [77,78]). The development of this facies starts after 6 ka BP and ends at about to 4 ka BP. The origin of this facies is not clear at present. Due to the absence of significant river inputs, it might assume a rise of fluids linked to the late hydrothermal phases of the Vulsino volcanism. Similar evidences were observed in the Specchio di Venere lake, a coastal basin in the volcanic island of Pantelleria (southern Sicily) [79].
- Shoreface Holocene facies (SH)—It is expressed by Unit 5. The presence of coastal malaco-ostracofauna partly reworked, shallow water oxidized foraminifera, as well as arenaceous pebbles and gravel levels, suggests that it is related to a shoreface environment. Locally (LB1), this environment could also be supplied by the remobilization of the Pleistocene sediments (CP facies) present at the inner edge of the depressed area.

The CP facies outcrops along the inner edge of the depression. At ESE of the Burano Lake, the CP facies deepens seawards (Figure 5). At WNW, the CP facies was not intercepted in the cores and therefore its seawards trend is not known. Stratigraphically overlapping on the CP facies, the LgH facies is present always with sharp contact. The chronological difference between the two facies highlights a sedimentary hiatus. The LgH facies shows a plane-concave geometry that tapers both seawards and landwards. The BdH facies, outcropping along the outer edge of the depression, constitutes the current Holocene beach-dune system. In the subsoil of south-eastern area, it displays a wedge geometry closed landward into LgH facies constituting a typical sand barrier. In the north-western area, the wedge geometry is only partially evident. The BdH and LgH facies are frequently heteropic and the relative contact is generally sharp or locally transitional. The LH facies presents a lenticular geometry and is

always embedded in the LgH one resulting heteropic with this. Regarding to SH facies, there is not enough information to define its geometry.

The characters of the facies and their mutual stratigraphic relations highlight the presence of two depositional sequences pro-parte (Figure 6) [80,81]. The oldest sequence (A) is represented only by the Upper Pleistocene CP facies. A second sequence (B), represented by Holocene facies, overlies sequence A. The overlap is identified along the surface separating the CP and LgH facies; this surface constitutes a *Basal Unconformity (BU)* (red line in Figure 6). The oldest sediments of LgH facies (about 8.0 to 6.0 ka BP), together with the heteropic sediments of BdH, show a typically transgressive setting associated with the Transgressive System Tract (TST) of the sequence B (Figure 6). Therefore, the *BU* surface therefore constitutes partly a *Transgressive Surface* (*TS*) in blue line in Figure 6. Most recent deposits of facies LgH and BdH display a regressive setting constituting the Highstand System Tract (HST) of the B sequence that develops above the *maximum flooding surface* (*mfs*) (yellow line in Figure 6). The HST of B sequence includes the LH facies embedded into LgH facies. Beyond the junction point of the *mfs* on the *BU*, the HST lagoon sediments of the B sequence lay directly on the A sequence.

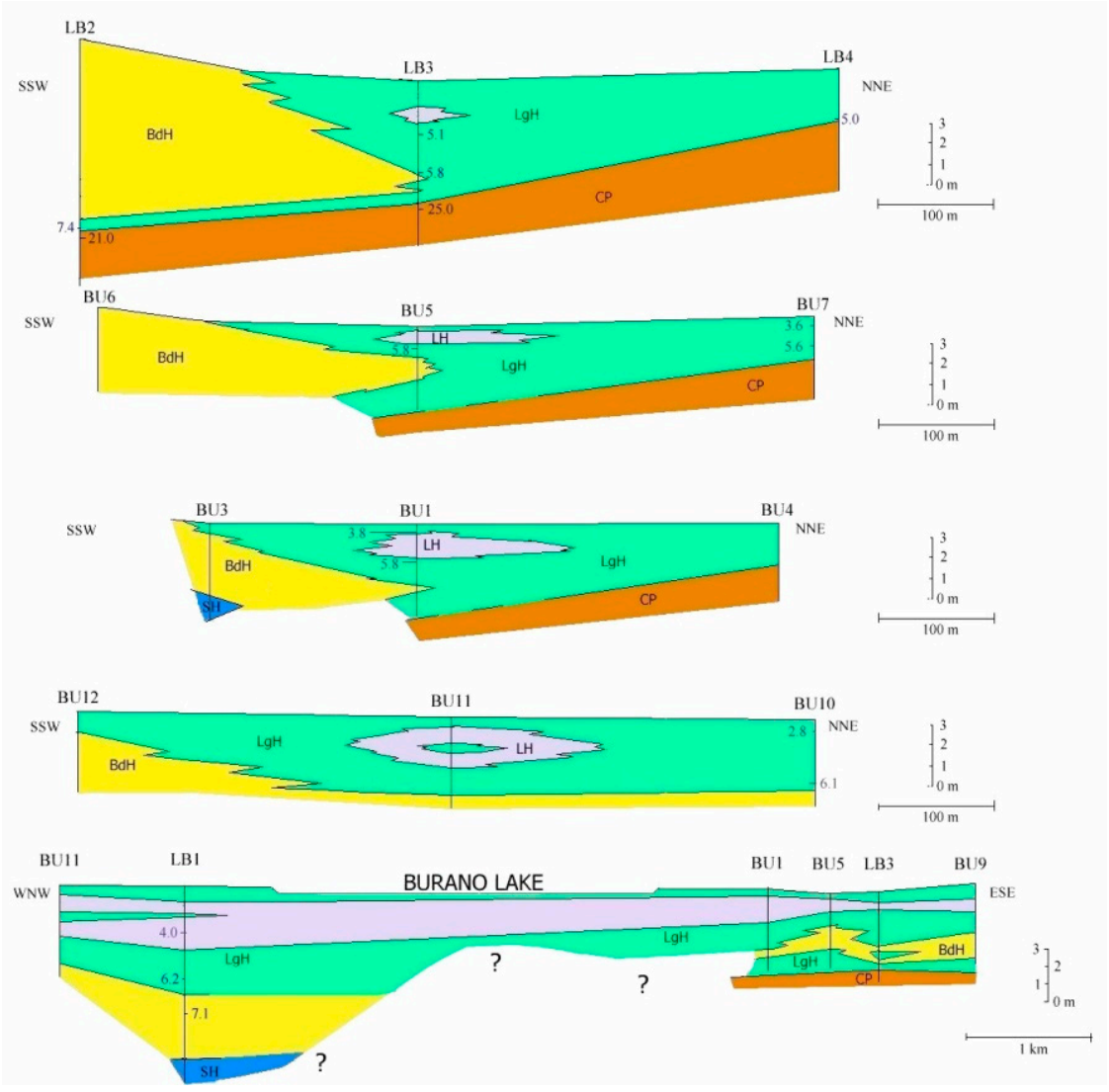

Figure 5. Schematic sedimentological cross-sections. Colours highlight the facies marked by relative label. For chronological reference, some ages approximate in ka BP was inserted.

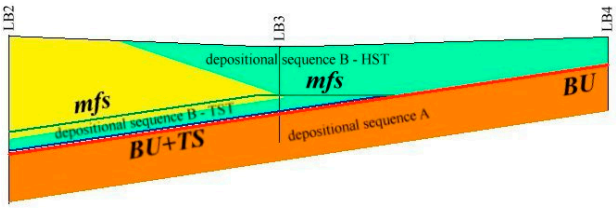

Figure 6. Sequence stratigraphy schematic setting. *BU* (red line): Basal Unconformity; *TS* (blue line): Transgressive Surface; *mfs* (green line): maximum flooding surface; TST: Transgressive System Tract; HST: High Stand System Tract. Depositional sequence A (brown) is constituted by coastal Pleistocene sediments. Depositional sequence B (TST + HST) is constituted by beach, bar and dune sediments (yellow) and lagoon/lacustrine sediments (light green).

5.2. Holocene Evolution

The paleoenvironmental history of the Burano paleo-lagoon can be summarized in 5 main phases starting from about 8000 years BP. This time interval includes the upper portion of the Neolithic up to the High Middle Ages, which largely centre the period characterized by increasing aridification phenomena (e.g., [9,82,83]). The vegetational and climate responses at the Mediterranean scale are documented by several palynological studies (e.g., [84–87] and references therein). Pollen data from the Burano paleo-lagoon show a prevalent warm temperate climate characterized by a quite humid weather conditions at least until about 4000 years BP despite the occurrence of greater seasonality phases. After 4000 years BP the significant increases of herbaceous cover, if not climate-induced, could be interpreted as an anthropogenic indicator of the impact of the Etruscan activities.

The RSL curve was drawn based on the calibrated ages from the sediments of the LgH and LH facies. Since the area is considered to be stable on average in the late-Quaternary, the curve was not corrected for the land vertical movements [88]. For each used data, the RSL was determined based on the equation RSL = A − RWL where: A is the altitude of the data (respect to the MSL) and RWL is a value equal to −0.5 (data from LgH facies) and 0 (data from LH facies) [89]. In Figure 7, the Burano RSL curve is compared with the RLS model curves of Sardinia [89] and Versilia plain [88]. These two locations have been considered as relatively close to the Burano area and considered on average stable.

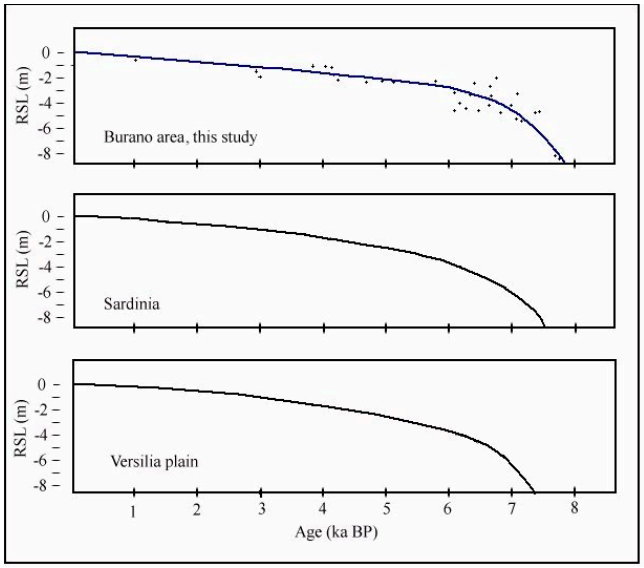

Figure 7. Comparison between the Burano RSL curve and the curves for Sardinia and Versilia plain modified from [88,89].

Phase 1 (Figure 8a)—In the easternmost sector of the study area, during the late transgression phase and before 7500 years BP, a sandy barrier (BdH) was located about 250 m seaward from the innermost shoreline consisting of Pleistocene sediments (CP). A narrow lagoon developed between the Pleistocene sediments and the sandy barrier (LgH) prone to seawater inflow. In the most western sector, the lagoon was not present and a large beach (facies BdH + SH) extended from the Pleistocene deposits seawards. The sandy barrier and beach were fed by the longshore current, carrying towards north-west the sediments from the Fiora, Arrone and Marta river mouths [90,91]. At this time, the sea level was close to −7 m when compared to the current one.

Phase 2 (Figure 8b)—About 6000 years ago, approximately at sea level still-stand, a barrier-lagoon system developed throughout the area. The boundary between the Pleistocene and Holocene deposits migrated to the northeast. The width of the lagoon varied from about 150 m in the eastern part to about 500 m in the western sector. There are no data that allow us to accurately evaluate the width of the barrier that even in the presence of washover events it began to limit the intrusion of seawater into the lagoon. During this phase, the sea level was about at −3 m compared to the current one.

Phase 3 (Figure 8c)—Even after the still stand, the sea level rose but with minor rates, and at around 5000 years BP, it was close to −2.5 m. In this phase, the width of the lagoon ranged from 500 to 700 m. The inner edge of the barrier shows a partial seaward migration in the eastern part. The LH facies occurs along the entire axis of the coastal basin.

Phase 4 (Figure 8d)—About 4000 years ago, the sea level was very close to −2 m. The planimetric features of the lagoon do not show a significant change in respect to the previous phase except for a limited seaward migration of the inner edge of the barrier in the westernmost part. However, the LH facies shows a more discontinuous distribution than the previous phase.

Phase 5—During the last 4000 years, LH facies disappeared and was overlain by limited thicknesses of LgH facies. Successively, the basin rapidly dried up, or, at least, turned into a wetland only locally and periodically submerged so that part of the organic sediments was subject to pedogenesis forming a thin brown soil. The reclamation made during the first part of the twentieth century, definitively dried up the entire area except the Burano Lake zone whose depth is currently not over a meter.

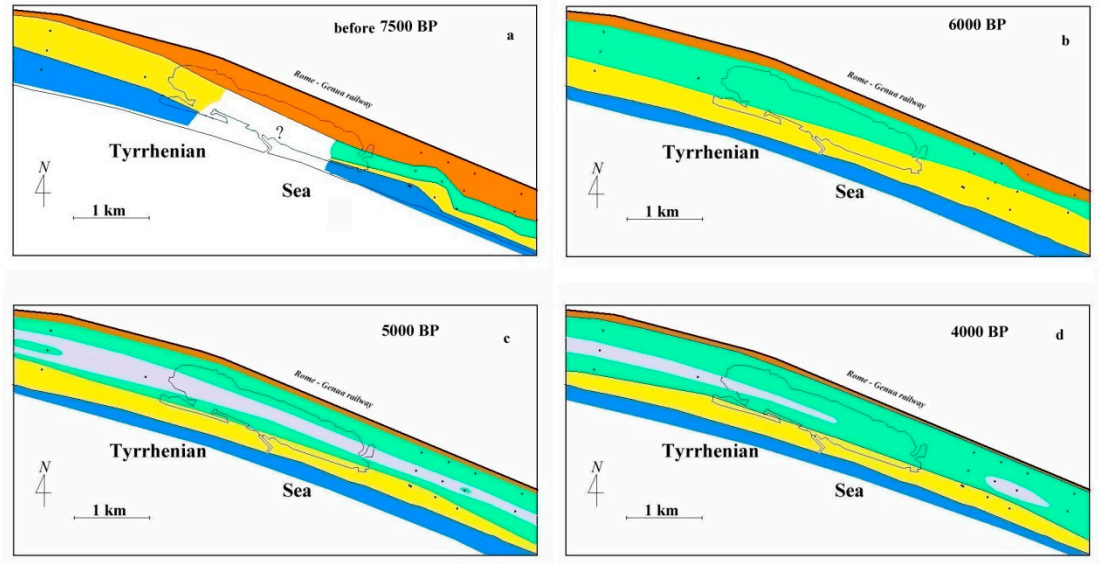

Figure 8. Schematic bidimensional landscape reconstructions of the Burano paleo-lagoon from 7500 to 4000 years BP (**a**–**d**). Coloured areas indicate: Pleistocene deposits (brown), lagoon/marsh Holocene deposits (green), Holocene sandy barrier and foreshore deposits (yellow), Holocene lacustrine deposits (grey), Holocene shoreface deposits (blue). The location of Burano Lake and the present shoreline is indicated.

6. Conclusions

A beach-dune-lagoon system evolved in the study area between about 8.0 and 4.0 ka BP, and it rests unconformably on the previous coastal sediments of Pleistocene age. In a first phase, the lagoon shows a significant marine influence and then, from 6000 years ago, it progressively changes to more closed environment with brackish water. Lagoon sediments are particularly rich in peat. Between 6.0 and 4.0 ka BP, along the central axis of the lagoon, a sedimentation particularly rich in $CaCO_3$ and bio indicators of freshwater-low brackish environment developed. From 4.0 ka BP ago, the lagoon quickly dried up becoming a locally and periodically submerged wetland. The area was reclaimed at the beginning of the 20th century.

Author Contributions: Conceptualization, M.D., P.B., A.B., L.D.B., C.V. and L.D.; Data curation, A.B., G.C., L.D.B., L.M.F., M.A.L., L.R., C.V., J.-P.G., L.S., P.C., F.P., C.O. and F.S.; Investigation, M.D., A.B., P.C.N., D.F., C.V. and J.-P.G.; Methodology, J.-P.G.; Supervision, P.B., L.D.B. and L.D. All authors have read and agreed to the published version of the manuscript.

Funding: This research received no external funding.

Acknowledgments: Fanny Guerin and Nora Dalal for their help in sieving samples from LB cores. Stoil Chapkanski (CNRS, Archéorient-UMR5133) and Camille Goncalves for the analysis of the Cosa samples. A special thanks to Maurizio Cacopardo for the collaboration during the drillings. We would like to thank SACRA Spa, in particular the Director Piergiorgio Santi, for the availability and collaboration shown, as well as for the authorization to carry out the mechanical drillings on the lands of the Company.

Conflicts of Interest: The authors declare no conflict of interest.

References

1. Kjerfve, B.; Magill, K.E. Geographic and hydrodynamic characteristics of shallow coastal lagoons. *Mar. Geol.* **1989**, *88*, 187–199. [CrossRef]
2. Dalrymple, R.W.; Leckie, D.A.; Tillman, R.W. Incised Valleys in time and space. *SEPM Publ.* **2006**, *85*, 343.
3. Marco-Barba, J.; Holmes, J.A.; Mesquita-Joanes, F.; Miracle, M.R. The influence of climate and sea level change on the Holocene evolution of a Mediterranean coastal lagoon: Evidence from ostracod palaeoecology and geochemistry. *Geobios* **2013**, *46*, 409–421. [CrossRef]
4. Marra, F.; Bozzano, F.; Cinti, F.R. Chronostratigraphic and lithologic feature soft the Tiber River sediments (Rome, Italy): Implications on the post-glacial sea-level rise and Holocene climate. *Glob. Planet. Chang.* **2013**, *107*, 157–176. [CrossRef]
5. Milli, S.; D'Ambrogi, C.; Bellotti, P.; Calderoni, G.; Carboni, M.G.; Celant, A.; Di Bella, L.; Di Rita, F.; Frezza, V.; Magri, D.; et al. The transition from wave-dominated estuary to wave -dominated delta: The Late Quaternary stratigraphic architeture of Tiber River deltaic succession (Italy). *Sediment. Geol.* **2013**, *284*, 159–180. [CrossRef]
6. Benallack, K.; Green, A.N.; Humphries, M.S.; Cooper, J.A.G.; Dladla, N.N.; Finch, J.M. The stratigraphic evolution of a large back-barrier lagoon system with a non-migrating barrier. *Mar. Geol.* **2016**, *379*, 64–77. [CrossRef]
7. Bortolin, E.; Weschenfelder, J.; Cooper, A. Holocene Evolution of Patos Lagoon, Brazil. *J. Coast. Res.* **2019**, *35*, 357–368. [CrossRef]
8. Dladla, N.N.; Green, A.N.; Cooper, J.A.G.; Humphries, M.S. Geological inheritance and its role in the geomorphological and sedimentological evolution of bedrock-hosted incised valleys, lake St Lucia, South Africa. *Estuar. Coast. Shelf Sci.* **2019**, *222*, 154–167. [CrossRef]
9. Mayewski, P.A.; Rohling, E.E.; Stager, J.C.; Karlen, W.; Maasch, K.A.; Meeker, L.D.; Meyerson, E.A.; Gasse, F.; Van Kreveld, S.; Holmgren, K.; et al. Holocene climate variability. *Quat. Res.* **2004**, *62*, 243–255. [CrossRef]
10. Vella, C.; Fleury, T.J.; Raccasi, G.; Provansal, M.; Sabatier, F.; Bourcier, M. Evolution of The Rhône delta plain in the Holocene. *Mar. Geol.* **2005**, *222*, 235–265. [CrossRef]
11. Mulligan, R.P.; Mallinson, D.J.; Clunies, G.J.; Rey, A.; Culver, S.J.; Zaremba, N.; Leorri, E.; Mitra, S. Estuarine Responses to Long-Term Changes in Inlets, Morphology, and Sea Level Rise. *J. Geophys. Res. Ocean.* **2019**, *124*, 12. [CrossRef]

12. Bellotti, P. Sedimentologia ed evoluzione olocenica della laguna costiera un tempo presente alla foce del Tevere. In Proceedings of the Atti del X Congresso Della Associazione Italiana di Oceanologia e Limnologia, Alassio, Italy, 4–6 November 1994.
13. Di Rita, F.; Celant, A.; Magri, D. Holocene environmental instability in the wetland north of the Tiber delta (Rome, Italy): Sea–lake–man interactions. *J. Paleolimnol.* **2010**, *44*, 51–67. [CrossRef]
14. Giraudi, C. The sediments of the 'Stagno di Maccarese' marsh (Tiber river delta, central Italy): A late-Holocene record of natural and human-induced environmental changes. *Holocene* **2011**, *21*, 1233–1243. [CrossRef]
15. Bellotti, P.; Calderoni, G.; Di Rita, F.; D'Orefice, M.; D'Amico, C.; Esu, D.; Magri, D.; Preite Martinez, M.; Tortora, P.; Valeri, P. The Tiber River delta plain (central Italy): Coastal evolution and implications for the ancient Ostia Roman settlement. *Holocene* **2011**, *21*, 1105–1116. [CrossRef]
16. Pannuzi, S. La laguna di Ostia: Produzione del sale e trasformazione del paesaggio dall'età antica all'età moderna. Available online: http://www.efrome.it/publications/resurce-en-ligne.html (accessed on 25 November 2013).
17. Vittori, C.; Mazzini, I.; Salomon, F.; Goiran, J.P.; Pannuzi, S.; Rossa, C.; Pellegrino, A. Palaeoenvironmental evolution of the ancient lagoon of Ostia Antica (Tiber delta, Italy). *J. Archaeol. Sci.* **2015**, *54*, 374–384. [CrossRef]
18. Davoli, L.; Raffi, R.; Baldassarre, A.M.; Bellotti, P.; Di Bella, L. New maps relative to the «Palude di Torre Flavia» (Central Tyrrhenian Sea-Italy) prone to severe coastal erosion. *IJEGE* **2019**, *2*, 13–21.
19. D'Orefice, M.; Graciotti, R.; Bertini, A.; Fedi, M.; Foresi, L.M.; Ricci, M.; Toti, F. Latest Pleistocene to Holocene environmental changes in the Northern Tyrrhenian area (central Mediterranean). A case study from southern Elba Island. *AMQ* **2020**, *33*, 1–25.
20. Goiran, J.P.; Pavlopoulos, K.P.; Fouache, E.; Triantaphyllou, M.; Etienne, R. Piraeus, the ancient island of Athens: Evidence from Holocene sediments and historical archives. *Geology* **2011**, *39*, 531–534. [CrossRef]
21. Stanley, D.J.; Bernasconi, M.P. Holocene depositional pattern and evolution in Alexandria's Eastern Harbor, Egypt. *J. Coast. Res.* **2006**, *22*, 283–297. [CrossRef]
22. Stanley, D.J.; Bernasconi, M.P. Sybaris-Thuri-Copia trilogy: Three delta coastal sites become landlocked. *Méditerranée* **2009**, *112*, 75–88. [CrossRef]
23. Bellotti, P.; Caputo, C.; Dall'Aglio, P.L.; Davoli, L.; Ferrari, K. Human settlement in an evolvine landscape. Man-environment interaction in the Sibari Plain (Ionian Calabria). *AMQ* **2009**, *22*, 61–72.
24. Bini, M.; Brückner, H.; Chelli, A.; Pappalardo, M.; Da Prato, S.; Gervasini, L. Palaeogeographies of the Magra Valley coastal plain to constrain the location of the Roman harbour of Luna (NW Italy). *Palaeogeogr. Palaeoclimatol. Palaeoecol.* **2012**, *337*, 37–51. [CrossRef]
25. Amorosi, A.; Bini, M.; Giacomelli, S.; Pappalardo, M.; Ribecai, C.; Rossi, V.; Sammartino, I.; Sarti, G. Middle to late Holocene environmental evolution of the Pisa plain (Tuscany, Italy) and early human settlements. *Quat. Int.* **2013**, *303*, 93–106. [CrossRef]
26. Anthony, E.J.; Marriner, N.; Morhange, C. Human influence and the changing geomorphology of Mediterranean deltas and coasts over last 6000 years: From progradation to destruction phase? *Earth Sci. Rev.* **2014**, *139*, 336–361. [CrossRef]
27. Ghilardi, M.; Istria, D.; Curras, A.; Vacchi, M.; Contreras, D.; Vella, C.; Dussouillez, P.; Crest, Y.; Guiter, P.; Delanghe, D. Reconstructing the landscape evolution and the human occupation of the Lower Sagone River (Western Corsica, France) from the Bronze Age to the Medieval period. *J. Archaeol. Sci.* **2017**, *12*, 741–754. [CrossRef]
28. Giaime, M.; Magne, G.; Bivolaru, A.; Gandouin, E.; Marriner, N.; Morhange, C. Halmyris. Geoarchaeology of a fluvial harbour on the Danube Delta (Dobrogea, Romania). *Holocene* **2018**, *28*, 1–15. [CrossRef]
29. Giaime, M.; Marriner, N.; Morhange, C. Evolution of ancient harbours in deltaic contexts: A geoarchaeological typology. *Earth Sci. Rev.* **2019**, *191*, 1–290. [CrossRef]
30. Regione Toscana. Carta Geologica Della Regione Toscana in Scala 1:10.000. 2015. Available online: http://www502.regione.toscana.it/geoscopio/cartoteca.html (accessed on 28 November 2014).
31. Bartole, R. Caratteri sismostratigrafici, strutturali e paleogeografici della piattaforma continentale tosco-laziale; suoi rapporti con l'Appennino settentrionale. *Boll. Soc. Geol. Ital.* **1990**, *109*, 599–622.
32. Servizio Geologico d'Italia—Carta Geologica d'Italia alla scala 1:100.000—Foglio 135 "Orbetello". 1968. Stab. L. Salomone, Roma. Available online: http://193.206.192.231/carta_geologica_italia/tavoletta.php?foglio=13501.02.2012 (accessed on 27 March 2020).

33. Carmignani, L.; Decandia, F.A.; Fantozzi, P.L.; Lazzaretto, A.; Lotta, D.; Meccheri, M. Tertiary extensional tectonics in Tuscany (Northern Apennines, Italy). *Tectonophysics* **1994**, *238*, 295–315. [CrossRef]
34. Bartole, R. The North Tyrrhenian-Northern Apennines post-collisional system: Constrain for a geodynamic model. *Terra Nova* **1995**, *7*, 7–30. [CrossRef]
35. Principe, C.; Malfatti, A.; Rosi, M.; Ambrosio, M.; Fagioli, M.T. Metodologia innovativa di carotaggio microstratigrafico: Esempio di applicazione alla tefrostratigrafia di prodotti vulcanici distali. *Geol. Tec. Ambient.* **1997**, *4*, 39–50.
36. Ambrosio, M.; Dellomonaco, G.; Fagioli, M.T.; Giannini, F.; Pareschi, M.T.; Pignatelli, L.; Rosi, M.; Santacroce, R.; Sulpizio, R.; Zanchetta, G. Utilizzo di fioretto meccanico e carotiere microstratigrafico inguainante per la valutazione degli spessori e della stratigrafia delle coltri vulcanoclastiche soggette a fenomeni di colata rapida di fango. *Geol. Tec. Ambient.* **1999**, *4*, 23–32.
37. Stuiver, M.; Polach, H.A. Discussion: Reporting of ^{14}C data. *Radiocarbon* **1977**, *19*, 355–363. [CrossRef]
38. Ramsey, B. *Oxcal V.3.10*; Research Laboratory for Archaeology: Oxford, UK, 2005.
39. Preusser, F.; Degering, D.; Fuchs, M.; Hilgers, A.; Kadereit, A.; Klasen, N.; Krbetschek, M.R.; Richter, D.; Spencer, J. Luminescence dating: Basics, methods and applications. *Quat. Sci. J.* **2008**, *57*, 95–149.
40. Murray, A.S.; Wintle, A.G. Luminescence dating of quartz using an improved single-aliquot regenerative-dose protocol. *Radiat. Meas.* **2000**, *32*, 57–73. [CrossRef]
41. Richter, D.; Richter, A.; Dornich, K. Lexsyg—A new system for luminescence research. *Geochronometria* **2013**, *40*, 220–228. [CrossRef]
42. Galbraith, R.F.; Roberts, R.G.; Laslett, G.M.; Yoshida, H.; Olley, J.M. Optical dating of single grains of quartz from Jinmium rock shelter, northern Australia. Part I: Experimental design and statistical models. *Archaeometry* **1999**, *41*, 339–364. [CrossRef]
43. Preusser, F.; Kasper, H.U. Comparison of dose rate determination using high-resolution gamma spectrometry and inductively coupled plasma-mass spectrometry. *Anc. tL* **2001**, *19*, 19–23.
44. Folk, R.L. Distinction between Grain Size and Mineral Composition in Sedimentary-Rocks Nomenclature. *J. Geol.* **1954**, *62*, 344–359. [CrossRef]
45. Murray, J.W. *Ecology and Applications of Benthic Foraminifera*; Cambridge University Press: Cambridge, UK, 2006; pp. 1–426. ISBN 978-051-153-552-9.
46. Hammer, O.; Harper, D.A.T.; Ryan, P.D. PAST: Paleontological Statistics Software Package for Education and Data Analisys. *Palaeontol. Electron.* **2001**, *4*, 1–9.
47. Loeblich, A.R., Jr.; Tappan, H. *Foraminiferal Genera and Their Classification*; Van Nostrand Reinhold Company: New York, NY, USA, 1988; pp. 1–71. ISBN 978-1-4899-5760-3.
48. Cimerman, F.; Langer, M. Mediterranean foraminifera. In *Slovenska Akademija Znanosti Umetnosti, Academia Scientiarum Artium Slovenica*; Classis IV: Ljubljana, Slovenia, 1991; pp. 1–118.
49. Sgarrella, F.; Moncharmont-Zei, M. Benthic foraminifera of the Gulf of Naples (Italy): Systematics and autoecology. *Boll. Soc. Paleontol. Ital.* **1993**, *32*, 145–264.
50. Milker, Y.; Schmiedl, G. A taxonomic guide to modern benthic shelf foraminifera of the western Mediterranean Sea. *Palaeontol. Electron.* **2012**, *15*, 1–134. [CrossRef]
51. WoRMS Editorial Board. World Register of Marine Species. Available online: http://www.marinespecies.orgatVLIZ (accessed on 2 December 2019).
52. Vittori, C. Trajectoires temporelles des environnements fluvio-lagunaires littoraux de la péninsule italique et sociétés anciennes. Ph.D. Dissertation, University of Strasbourg, Strasbourg, France, 2020.
53. Bonaduce, G.; Ciampo, G.; Masoli, M. Distribution of ostracoda in the Adriatic Sea. *Pubbl. Stn. Zool. Napoli* **1975**, *40*, 1–304.
54. Bonaduce, G.; Masoli, M.; Pugliese, N. Ostracodi bentonici dell'alto Tirreno. *Sci. Nat. Acta Biol.* **1977**, *54*, 243–261.
55. Athersuch, J.; Horne, D.J.; Whittaker, J.E. *Marine and Brackish Water Ostracods (Superfamilies Cypridacea and Cytheracea): Key and Notes for Identification of Species*; Synopsis of the British Fauna (New Series) 43; The Linnean Society of London and the Estuarine and Brackish-Water Sciences Association: Leiden, UK, 1989.
56. Meisch, C. Freshwater ostracoda of Western and Central Europe. In *Süsswasserfauna von Mitteleuropa 8/3*; Schwoerbel, J., Zwick, P., Eds.; Spektrum Akademischer Verlag: Heidelberg, Germany, 2000; pp. 1–522. ISBN 978-1-4020-6417-3.

57. Faranda, C.; Gliozzi, E. The ostracod fauna of the Plio-Pleistocene Monte Mario succession (Roma, Italy). *Boll. Soc. Paleontol. Ital.* **2008**, *47*, 215–267.
58. Fuhrmann, R. *Atlas Quartärer und Rezenter Ostrakoden Mitteldeutschlands*; Altenburger Naturwissenschaftliche Forsc-hungen: Altenburg, Germany, 2012.
59. Aiello, G.; Barra, D.; Parisi, R.; Isaia, R.; Marturano, A. Holocene benthic foraminiferal and ostracod assemblages in a paleo-hydrothermal vent system of Campi Flegrei (Campania, South Italy). *Palaeontol. Electron.* **2018**, *21*, 41. [CrossRef]
60. Ruiz, F.; Abad, M.; Galán, E.; González, I.; Aguilá, I.; Olías, M.; Gómez Ariza, J.L.; Cantano, M. The present environmental scenario of El Melah Lagoon (NE Tunisia) and its evolution to a future sabkha. *J. Afr. Earth Sci.* **2006**, *44*, 289–302. [CrossRef]
61. Salel, T.; Bruneton, H.; Lefèvre, D. Ostracods and environmental variability in lagoons and deltas along the north-western Mediterranean coast (Gulf of Lions, France and Ebro delta, Spain). *Rev. Micropaléontologie* **2016**, *59*, 425–444. [CrossRef]
62. Arbulla, D.; Pugliese, N.; Russo, A. Ostracods from the National Park of La Maddalena Archipelago (Sardinia, Italy). *Boll. Soc. Paleontol. Ital.* **2004**, *43*, 91–99.
63. Ruiz, F.; González-Regalado, M.L.; Baceta, J.I.; Menegazzo-Vitturi, L.; Pistolato, M.; Rampazzo, G.; Molinaroli, E. Los ostrácodos actuales de la laguna de Venecia (NE de Italia). *Geobios* **2000**, *33*, 447–454. [CrossRef]
64. Mansouri, R.; Bobier, C.; Carbonel, P.; Tastet, J.P. Contribution à la connaissance des systèmes lagunaires en domaine méditerranéen: Les milieux actuels et les paléoenvironnements du lac de Ghar El Melh et de la sebkha de l'Ariana (Tunisie). *Boll. Oceanol. Teor. Appl.* **1985**, *3*, 167–195.
65. Mazzini, I.; Rossi, V.; Da Prato, S.; Ruscito, V. Ostracods in archaeological sites along the Mediterranean coastlines: Three case studies from the Italian peninsula. In *The Archaeological and Forensic Applications of Microfossils: A Deeper Understanding of Human Histo*; Williams, M., Hill, T., Eds.; The Micropalaeontological Society, Special Publications. Geological Society: London, UK, 2017; pp. 121–142. ISBN 178-620-305-7.
66. Triantaphyllou, M.V.; Kouli, K.; Tsourou, T.; Koukousioura, O.; Pavlopoulos, K.; Dermitzakis, M.D. Paleoenvironmental changes since 3000 BC in the coastal marsh of Vravron (Attica, SE Greece). *Quat. Int.* **2010**, *216*, 14–22. [CrossRef]
67. Koukousioura, O.; Dimiza, M.D.; Kyriazidou, E.; Triantaphyllou, M.V.; Syrides, G.; Aidona, E.; Vouvalidis, K.; Panagiotopoulos, I.; Papadopoulou, L. Environmental evolution of the Paliouras coastal lagoon in the eastern Thermaikos gulf (Greece) during Holocene. *Environ. Earth Sci.* **2019**, *78*. [CrossRef]
68. Debenay, J.P.; Guillou, J.J. Ecological Transitions Indicated by Foraminiferal Assemblages in Paralic Environments. *Estuaries* **2002**, *25*, 1107–1120. [CrossRef]
69. Laut, L.; Silva, F.S.; Figueiredo, A.G., Jr.; Laut, V. Assembleias de foraminíferos e tecamebas associadas a análises sedimentológicas e microbiológicas no delta do rio Paraíba do Sul, Rio de Janeiro, Brasil. *Pesqui. Geociências* **2011**, *38*, 251–267. [CrossRef]
70. Martins, A.M.V.; Zaaboub, N.; Aleya, L.; Frontalini, F.; Pereira, E.; Miranda, P.; Mane, M.; Rocha, F.; Laut, L.; El Bour, M. Environmental Quality Assessment of Bizerte Lagoon (Tunisia) Using Living Foraminifera Assemblages and a Multiproxy Approach. *PLoS ONE* **2015**, *10*, e0137250. [CrossRef]
71. Belart, P.; Frontalini, F.; Laut, V.; Fortes, R.; Clemente, I.; Raposo, D.; Martins, V.; Lorini, M.L.; Rocha Fortes, R.; Laut, L. Living benthic Foraminifera from the Saquarema lagoonal system (Rio de Janeiro, southeastern Brazil). *Check List* **2017**, *13*, 1–2062. [CrossRef]
72. Zonneveld, K.A.F.; Marret, F.; Versteegh, G.J.M.; Bogus, K.; Bonnet, S.; Bouimetarhan, I.; Crouch, E.; de Vernal, A.; Elshanawany, R.; Edwards, L.; et al. Geographic distribution of dinoflagellate cysts in surface sediments. *Pangaea* **2013**. [CrossRef]
73. Dimiza, M.D.; Koukousioura, O.; Triantaphyllou, M.V.; Dermitzakis, M.D. Live and dead benthic foraminiferal assemblages from coastal environments of the Aegean Sea (Greece): Distribution and diversity. *Rev. Micropaléontologie* **2016**, *59*, 19–32. [CrossRef]
74. Batten, D.J.; Grenfell, H.R. Green and blue-green algae. *Palynol. Princ. Appl.* **1996**, *36*, 205–214.
75. Guy-Ohlson, D. *Botryococcus* as an aid in the interpretation of palaeoenvironment and depositional processes. *Rev. Palaeobot. Palynol.* **1992**, *71*, 1–15. [CrossRef]
76. Tyson, R.V. Distribution of the palynomorph group: Phytoplankton subgroup, chlorococcale algae. In *Sedimentary Organic Matter*; Springer: Dordrecht, The Netherlands, 1995.

77. Castro Alonso, M.J.; Montañez Hernández, L.E.; Sanchez Muñoz, M.A.; Franco, M.; Rubi, M.; Narayanasamy, R.; Balagurusamy, N. Microbially Induced Calcium carbonate Precipitation (MICP) and its potential in Bioconcrete: Microbiological and molecular concepts. *Front. Mater.* **2019**, *6*, 1–126. [CrossRef]
78. Karami, F.; Balci, N.; Guven, B. A modeling approach for calcium carbonate precipitation in a hypersaline environment: A case study from a shallow, alkaline lake. *Ecol. Complex.* **2019**, *39*, 100–774. [CrossRef]
79. Cangemi, M.; Bellanca, A.; Borin, S.; Hopkinson, L.; Mapelli, F.; Neri, R. The genesis of actively growing siliceous stromatolites: Evidence from Lake Specchio di Venere, Pantelleria Island, Italy. *Chem. Geol.* **2010**, *276*, 318–330. [CrossRef]
80. Posamentier, H.W.; Vail, P.R. Eustatic Controls on Clastic Deposition II: Sequence and Systems Tract Models. In *Sea Level Change: An Integrated Approach*; Wilgus, C.K., Hastings, B.S., Eds.; SEPM Publ.: Tulsa, OK, USA, 1988; pp. 125–154. ISBN 978-091-898-574-3.
81. Posamentier, H.W.; Allen, G.P. Siliciclastic sequence stratigraphy—Concepts and applications. *Sedimentol. Paleontol.* **1999**, *7*, 210.
82. Roberts, N.; Brayshaw, D.; Kuzucuoğlu, C.; Perez, R.; Sadori, L. The mid-Holocene climatic transition in the Mediterranean: Causes and consequences. *Holocene* **2011**, *21*, 3–13. [CrossRef]
83. Bini, M.; Zanchetta, G.; Perşoiu, A.; Cartier, R.; Català, A.; Cacho, I.; Dean, J.R.; Di Rita, F.; Drysdale, R.N.; Finnè, M.; et al. The 4.2 ka BP Event in the Mediterranean region: An overview. *Clim. Past* **2019**, *15*, 555–577. [CrossRef]
84. Currás, A.; Ghilardi, M.; Peche-Quilichini, K.; Fagel, N.; Vacchi, M.; Delanghe, D.; Dussouillez, P.; Vella, C.; Bontempi, J.M.; Ottaviani, J.C. Reconstructing past landscapes of the eastern plain of Corsica (NW Mediterranean) during the last 6000 years based on molluscan, sedimentological and palynological analyses. *J. Archaeol. Sci. Rep.* **2017**, *12*, 755–769. [CrossRef]
85. Di Rita, F.; Fletcher, W.J.; Aranbarri, J.; Margaritelli, G.; Lirer, F.; Magri, D. Holocene forest dynamics in central and western Mediterranean: Periodicity, spatio-temporal patterns and climate influence. *Sci. Rep.* **2018**, *8*, 8929. [CrossRef]
86. Melis, R.T.; Depalmas, A.; Di Rita, F.; Montisa, F.; Vacchi, M. Mid to late Holocene environmental changes along the coast of western Sardinia (Mediterranean Sea). *Glob. Planet. Chang.* **2017**, *155*, 29–41. [CrossRef]
87. Sadori, L.; Koutsodendris, A.; Panagiotopoulos, K.; Masi, A.; Bertini, A.; Combourieu-Nebout, N.; Francke, A.; Kouli, K.; Joannin, S.; Mercuri, A.M.; et al. Pollen data of the last 500 ka BP at Lake Ohrid (south-eastern Europe). PANGAEA. Supplement to 2016, Pollen-based paleoenvoronmental and paleoclimatic change at Lake Ohrid (south-eastern Europe) during the past 500 ka. *Biogeosciences* **2018**, *13*, 1423–2016. [CrossRef]
88. Lambeck, K.; Antonioli, F.; Anzidei, M.; Ferranti, L.; Leoni, G.; Scicchitano, G.; Silenzi, S. Sea level change along the Italian coast during the Holocene and projections for the future. *Quat. Int.* **2011**, *232*, 250–257. [CrossRef]
89. Vacchi, M.; Ghilardi, M.; Melis, R.T.; Spada, G.; Giaime, M.; Marriner, N.; Lorscheid, T.; Morhange, C.; Burjachs, F.; Rovere, A. New relative sea-level insights into the isostatic history of the Western Mediterranean. *Quat. Sci. Rev.* **2018**, *201*, 396–408. [CrossRef]
90. Bartolini, C.; Corda, L.; D'Alessandro, L.; La Monica, G.B.; Regini, E. Studi di Geomorfologia costiera: III—Il tombolo di Feniglia. *Boll. Soc. Geol. Ital.* **1979**, *96*, 117–157.
91. Evangelista, S.; Full, W.E.; Tortora, P. Provenance and dispersion of fluvial, beach and shelf sands in the bassa Maremma coastal system (central Italy): An integrated approach using Fourier shape analysis, grain size and seismic data. *Boll. Soc. Geol. Ital.* **1996**, *115*, 195–217.